JOURNAL OF POLYMER SCIENCE | PART B

Polymer Physics

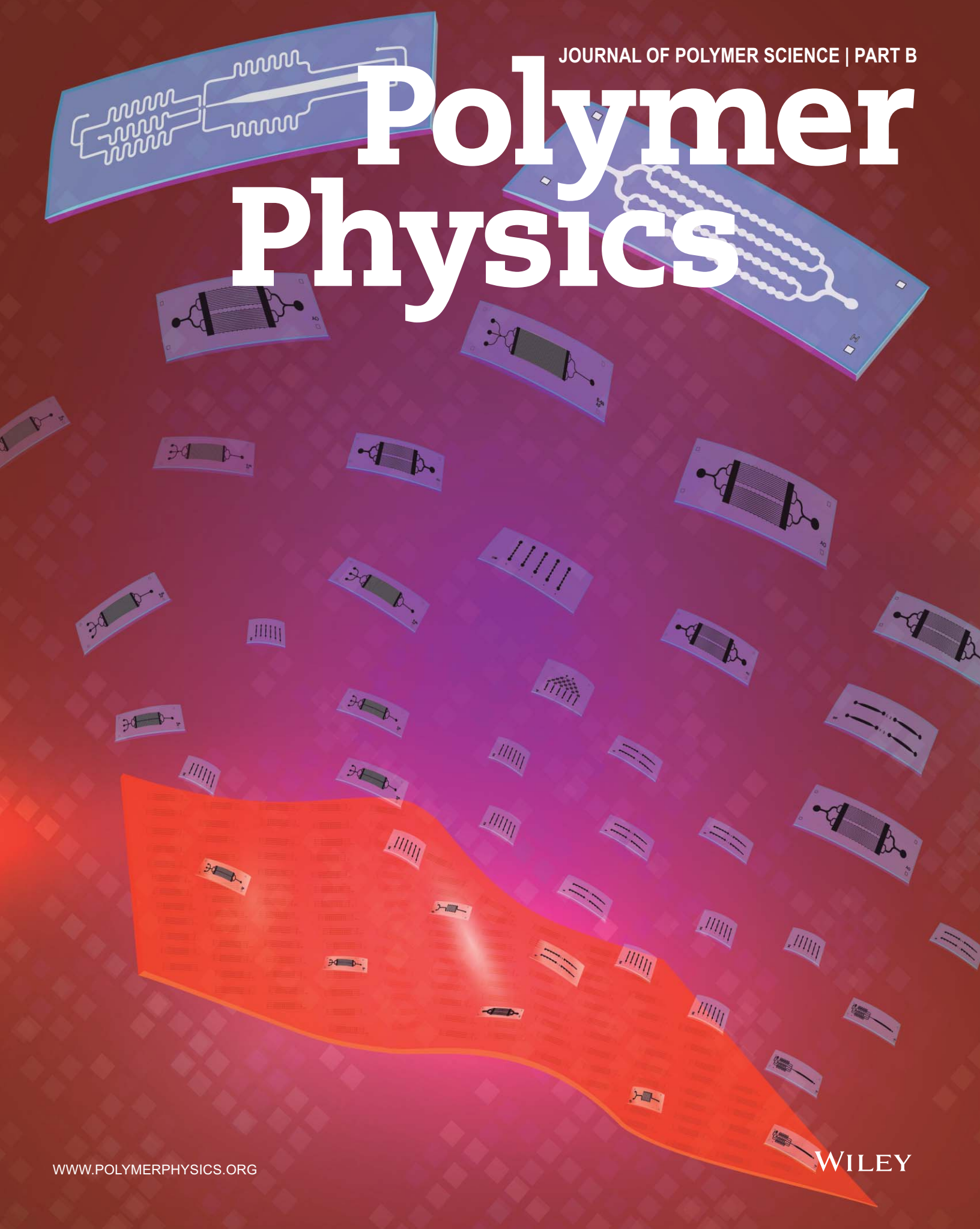

WWW.POLYMERPHYSICS.ORG

WILEY

Accessible and Cost-Effective Method of PDMS Microdevices Fabrication Using a Reusable Photopolymer Mold

Natalia Bourguignon,[1] Carol M. Olmos,[1] Marina Sierra-Rodero,[1] Ana Peñaherrera,[1] Gustavo Rosero,[1] Pedro Pineda,[1] Karla Vizuete,[2] Carlos R. Arroyo,[2] Luis Cumbal,[2] Carlos Lasorsa,[1] Maximiliano S. Perez,[1,3] Betiana Lerner [1,3]

[1]Facultad Regional Haedo, Universidad Tecnológica Nacional (UTN), Haedo, E 1706, Buenos Aires, Argentina
[2]Centro de Nanociencia y Nanotecnología, Universidad de las Fuerzas Armadas ESPE, Sangolqui, P.O. Box 171-5-231B, Ecuador
[3]Instituto de Ingeniería Biomédica, Universidad de Buenos Aires (UBA), Buenos Aires, C1063ACV, Argentina
Correspondence to: B. Lerner (E-mail: blerner@frh.utn.edu.ar); M. Perez (E-mail: max@fullgen.com)

Received 23 April 2018; accepted 20 July 2018
DOI: 10.1002/polb.24726

ABSTRACT: This work describes a novel and cost-effective method of polydimethylsiloxane (PDMS) microchips fabrication by using a printing plate photopolymer called Flexcel as a master mold (Fmold). This method has demonstrated the ability to generate multiple devices from a single master, reaching a minimum channel size of 25 μm, structures height ranging from 53 to 1500 μm and achieving dimensions of 1270 × 2062 mm^2, which are larger than those obtained by the known techniques to date. Scanning electron microscopy, atomic force microscopy, and profilometry techniques have been employed to characterize the Fmold and PDMS replicas. The results showed high replication fidelity of Fmold to the PDMS replica. Furthermore, it was proved the reusability of the Fmold. In our study, up to 50 PDMS replicas have been fabricated without apparent degradation of the mold. The feasibility of the resulting PDMS replica was effectively demonstrated using a microfluidic device for enhanced oil recovery analysis. © 2018 Wiley Periodicals, Inc. J. Polym. Sci., Part B: Polym. Phys. **2018**

KEYWORDS: enhanced oil recovery; PDMS microchips fabrication; printing plate photopolymer mold

INTRODUCTION Polydimethylsiloxane (PDMS) is a widely used material in the manufacture of microfluidic devices, because this transparent elastomer offers chemical resistance and biocompatibility.[1] Besides, PDMS devices are easy to fabricate and enables a wide range of applications.[1] PDMS microdevices are mostly fabricated via soft lithography technology,[2] being the SU-8 the most common photoresist used for this purpose.[3] This technique allows the creation of microstructures with high resolution (~1 μm).[4] However, it has several significant disadvantages: the molds normally use silicon wafers as substrates which are fragile, their size is limited (normally not wider than 4 or 6 in.), and the photoresin is prone to delamination.[4] In addition, SU-8 molds fabrication requires clean room facilities, which are not available in all countries, limiting their use only to laboratories that have access to expensive equipment to generate the masks and perform the lithographic processes.

The increasing of the lab-on-a-chip applications in various research fields brings the opportunity to develop new low-cost and high feasibility methodologies for PDMS microdevices fabrication. The literature reports many alternative fabrication techniques that do not require lithography such as thermoplastic building blocks,[5] toner transfer masking,[6] wax molds,[7,8] liquid molding,[9,10] laser ablation and reusable PDMS molds,[11] laser swelling,[12] semicontact-writing,[13] stainless steel stamps,[14] capillary forming,[15] printing plate photopolymers,[16] and transfer printing.[17] However, most of these techniques do not achieve the resolution of the photoresins or the processes are expensive.

The motivation of this work has been the fabrication of PDMS devices for enhanced oil recovery (EOR) studies, by using an alternative cost-effective method that does not require lithography. In the last few years, there is a growing interest in the use of microdevices for EOR assays. EOR microfluidic devices offer a new test methodology that quickly provides information about potential compounds in upstream oil exploration and production, allowing a better understanding of the mechanisms of action of fluids in a reservoir.[18,19] Microfluidic

Additional Supporting Information may be found in the online version of this article.

Natalia Bourguignon and Carol M. Olmos contributed equally to this work.

© 2018 Wiley Periodicals, Inc.

devices for EOR methods have several advantages such as cost-effectiveness, reproducibility, low-volume requirements, simple and precise display, speed of testing, and versatility of designs and portability.[20] EOR essays also provide a positive environmental impact, since less reactive chemicals are consumed in the current routine tests, with the consequent reduction in laboratory waste. Karadimitriou and Hassanizadeh explained in detail the microfabrication methods for studying two-phase flow in porous media and the relevance of microfluidic systems for EOR.[20] Microfabrication offers new ways for the study of EOR processes by designing and manufacturing microsystems that mimic porous rock formations, because the pore length in the oil-bearing rocks is at the microscale range.[21]

In this work, a simple and accessible process for the fabrication of PDMS microdevices by using a mold from printing plate photopolymer has been developed. The photopolymer called Flexcel allowed the fabrication of master molds with dimensions up to 1270 × 2062 mm^2, structure heights ranging from 53 to 1500 μm, precise dimensions, and a reproduction of a minimum dot of 10 μm. The reproduction fidelity, stability, and durability of the photopolymeric mold (Fmold) were tested producing up to 50 PDMS replicas. Surface morphological features of the Fmold and PDMS replicas were examined by scanning electron microscopy (SEM), atomic force microscopy (AFM), and profilometry. As a proof of concept, the fabrication and testing of microfluidic devices for EOR assays was performed.

EXPERIMENTAL

Fmold Fabrication

The printing plate photopolymer Flexcel SRH and DITR film used in the fabrication of molds (Fmold) were supplied by Eastman Kodak.[22] Sheets of 1270 × 2062 mm^2 of Flexcel SRH and DITR film were chosen for the fabrication of molds. The photopolymer thickness was around 1.14 mm.[23] The flexographic plate usually composed of an elastomeric, styrene–diene–styrene-based photo polymeric sheet on a polyethylene terephthalate base[24,25] was solvent washable or water washable. The organic compounds were crosslinked by the exposure to UVA wavelengths as crosslinker initiators and UVC wavelengths were used to end the reaction, giving large and stable molecular structures insoluble in the defined developing solution.

For the Fmold fabrication (Figure 1), microchannel network was designed with Layout editor software,[26] the design was transferred to the DITR film with an infrared laser source of 2400 ppi. Then, the film was laminated onto the unexposed flexographic printing plate before being exposed to UVA light at 0.45 J on the reverse side and UVA light at 19 J on the front for 360 s. The time of UVA exposure on the reverse side varies during the process. After the exposure, the film was removed. Then, the flexographic printing plate was washed with solvent PROSOL N-1 at 360 mm min^{-1} and dried in an oven during 30 min at 50°C.

In the last step, the flexographic printing plate was exposed to UVC light at 10 J for 17 min and UVA light at 4 J for 2 min on the front. The same procedure was applied to prepare the Fmold used to fabricate the PDMS-floor replica, without layout design application.

The Fmold obtained was then covered with an ultrathin SiO_2 film by plasma-enhanced chemical vapor deposition (PEVCD). PECVD homemade reactor provided an electric continuous power source of glow discharge of 900 V with capacitive coupling and impedance matching. The vacuum chamber was made with a Pyrex glass tube of 80 cm long and 15 cm diameter. Hexamethyldisilazane (HMDS) (Dow Corning) was used as a precursor monomer. The working gas (O_2) entry was located at the end of the vacuum chamber, far from the substrate, allowing vapor ionization in the area of discharge generation and SiO_2 coating production. The coating process was performed according to the conditions described by Lasorsa et al.[27] The PEVCD working conditions were 8 mL s^{-1} O_2 flow rate, 1 mbar gas pressure and 3 h exposure time. Note that Fmold without any treatment is referred as Fmold and the mold covered with an ultrathin SiO_2 film is called as Fmold-T (SiO_2 treated).

PDMS Microdevice Fabrication

PDMS microdevices (Sylgard 184, Dow Corning, USA) were fabricated as previously described by Peñaherrera et al.[28] Briefly, PDMS was mixed with curing agent in a 10:1 ratio. Then, the mixture was placed under vacuum to remove air bubbles, poured onto the Fmold-T and cured in an oven at 40°C overnight. Before fabrication of each PDMS device, the Fmold-T was silanized using trichloro(1H,1H,2H,2H-perfluorooctyl)silane (Sigma-Aldrich, Argentina) via vapor deposition under vacuum.

After curing, the PDMS replica was peeled off from the mold and holes were punched in order to connect it externally to syringe pump (ADOX—AcTIVA A22). To assemble the microfluidic device, the PDMS replica was irreversibly bonded to a PDMS-floor replica by exposure to oxygen plasma carried out in the PECVD reactor. The PDMS surfaces were first activated by O_2 plasma (900 V, 1 mbar, 30 s) to create the -SiOH group on the PDMS surface. After the surface activation, the PDMS replicas were placed in contact immediately.

Characterization

The surface morphology of the Fmolds and PDMS replicas was determined using a field emission gun SEM (TESCAN FEG SEM MIRA3). In order to avoid samples damage, SEM measurements were carried out at voltages between 3 and 5 kV. Previously, the molds were metalized with an approximately 20 nm thick gold layer. Fmold roughness was determined via AFM (Dimension Icon with ScanAsyst, Bruker, Ecuador). AFM images were acquired in ScanAsyst mode at ambient conditions by using a cantilever of spring constant at 0.71 N/m. The average roughness (Ra) parameter was determined by applying the Nanoscope Analysis 1.8 software to multiple images taken at random positions in scan areas of

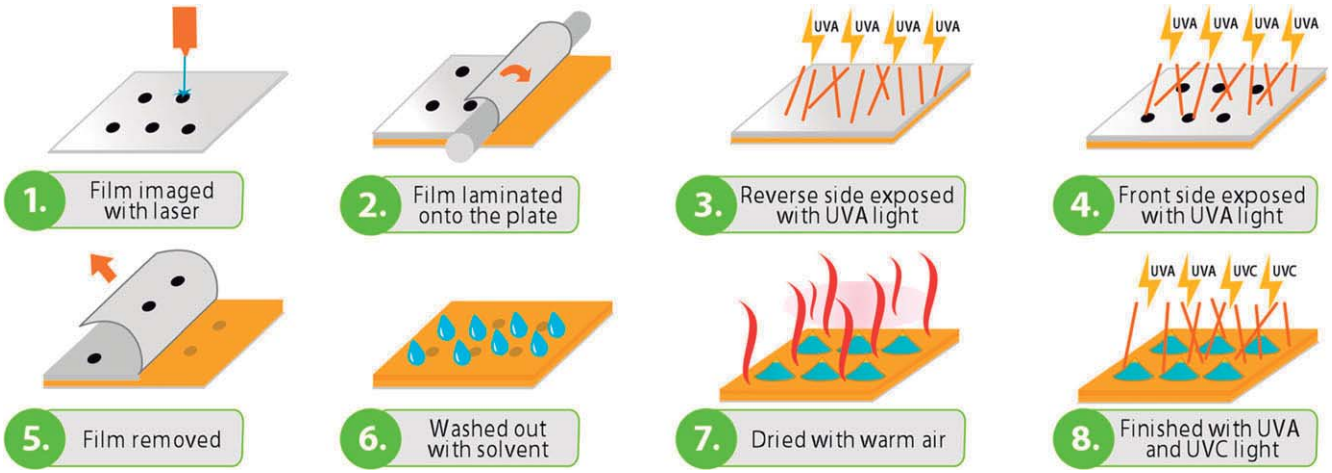

FIGURE 1 Fmold method fabrication. [Color figure can be viewed at wieyonlinelibrary.com]

$50 \times 50\ \mu m^2$. AFM images reported in this work were reproducible over at least five points on the sample surface. Profilometry measurements were performed using Dektak XT profilometer from Bruker and the analysis was carried out using the Vision 64 software. The images of the Fmolds and PDMS microdevices were taken with a binocular magnifier (Biotraza) attached to a digital camera.

Applications

In order to test the usefulness of the proposed Fmold methodology for PDMS microdevices fabrication, microfluidic chips were designed and employed for EOR applications. Figure 2 shows the design of the microfluidic device used for EOR experiments. Porosity, poral volume (PV) and height correspond to 32%, 22 μL, and 81 μm, respectively. The pore throat sizes are 400 and 650 μm.

The oil recovery experiment was performed using crude oil, deionized water with acid blue dye, and polyacrylamide polymer (1000 ppm). The crude oil used in this experiment has a density of 0.81 g mL^{-1} and a viscosity of 4.42 cP at 25°C. Before injection of oil into the microfluidic device, its impurities were removed by rotating the oil in a centrifuge. A binocular magnifier was used to observe the flow inside the channel, and a Canon T3-I Rebel digital camera attached to the loupe recorded the phenomena. Images from the experiment were obtained and the analysis was performed using Fiji by Image J software.[29]

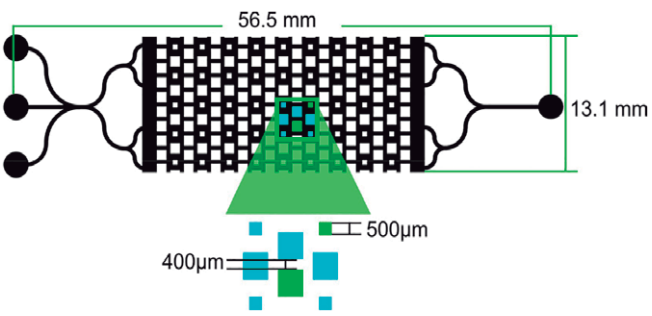

FIGURE 2 Design of microfluidic device for EOR experiment. [Color figure can be viewed at wieyonlinelibrary.com]

RESULTS AND DISCUSSION

The first major goal of this contribution was to provide an accessible and cost-effective alternative to fabricate PDMS microdevices compared to conventional methods. Data obtained through mold characterization provided information for its application in microfluidic field such as EOR assays.

Mold Characterization

Figure 3 shows the structures height as a function of scanning length. The UVA exposure during 35, 40, and 48 s generated molds with heights of 297, 211 and 81 μm, respectively. Based on these results, an inverse relationship between UVA exposure time and structure height is demonstrated.

Furthermore, the effect of the UVA exposure time on the surface morphology was studied by measuring the roughness of Fmolds. AFM images and the corresponding average roughness (Ra) values are presented in Figure 4. The AFM images and roughness values show that surface changes by the effect of UVA exposure time.

The order of Ra parameter values are: A: 23 nm (35 s) < B: 30.9 nm (40 s) < C: 99.9 nm (48 s). The Fmold C is much rougher than the Fmold B and A. Specifically, changes on the Fmold surface roughness can be attributed to changes on the crosslinking degree in the material,[30] as well as modifications in the type of bonds in the surface layer[31] caused by the UVA treatment. In comparison with other traditional molds, Fmold presents higher roughness than the SU-8 resin (~10 nm)[32] but lower than mold roughness manufactured by 3D Systems (~2 μm),[33,34] micromilling (~0.5 μm),[33] and laser ablation (~7 μm).[33,35]

It was found a direct dependency between UVA exposure and roughness of the surface and, in contrast, a prolonged UVA radiation causes the decrease of height (Figure 5). These results provide valuable information of surface properties,

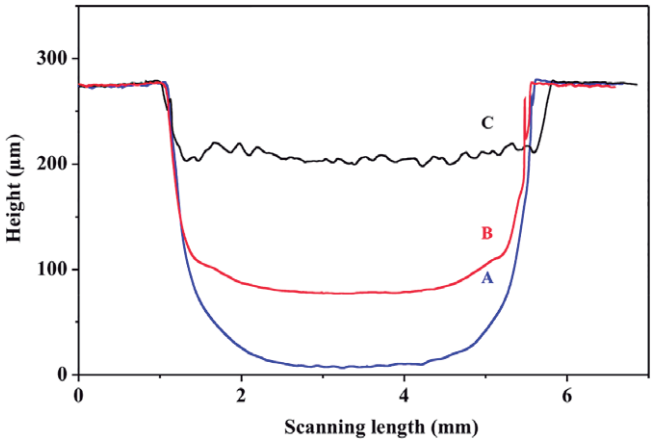

FIGURE 3 Height measurements of structures formed in Fmold. UVA exposure time on reverse side: A: 35 s, B: 40 s, and C: 48 s. Height measurements were determined by profilometry technique ($n = 3$). [Color figure can be viewed at wieyonlinelibrary.com]

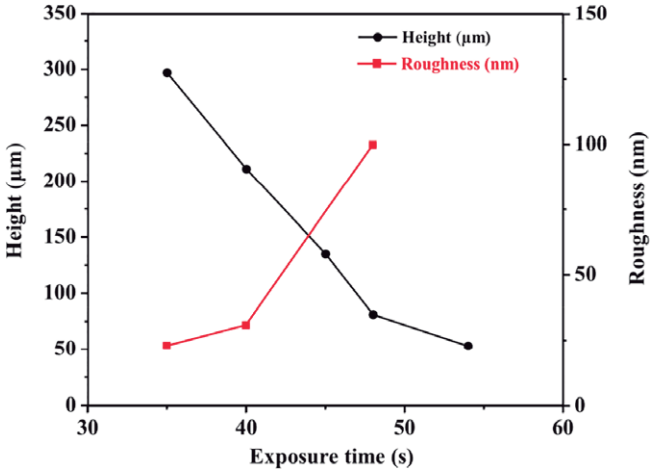

FIGURE 5 Effect of reverse side UVA exposure times on the height of structures and surface roughness. Black line: height of the structures. Red line: roughness. [Color figure can be viewed at wieyonlinelibrary.com]

which is relevant on the application of the microfluidic devices. Fmolds with dimensions of a standard test target USAF 1951[36] were fabricated by applying UVA exposure time on reverse side at times of 54 and 45 s, obtaining height measurements corresponding to 53 and 135 μm, respectively. These measurements are included in Figure 5 and in Figure S1, Supporting Information.

Figure 6 shows SEM images of Fmold with rectangular structures and dimensions acquired from the standard test target USAF 1951. The structures width designed with Layout editor software resulted in the range between 10 and 520 μm. The images indicate uniformly distributed rectangular forms, with structures ranging from 25 to 520 μm. SEM images of Fmold evidences the inclination of the structures sidewalls. Besides, widths less than 25 μm were not resolved. The relationship of the sidewalls inclination with UV exposure has been previously reported by Liu et al.[37] demonstrating the proportionality between face exposure and the shoulder angle.

Structure height uniformity was tested by profilometry. Figure 7 shows that height of structures assigned in the figure as 1–9 exhibit an average of 53 μm, whereas the structures 10 and 11 show values of 42 and 38 μm, respectively. The differences of heights are due to the inclination of the structures, causing an overlapping.

Figure 8(a,b) shows SEM images of the cross section of the Fmold, observing trapezoidal shapes on the structures. This characteristic shape generates an overlapping of continuous structures as shown in the schematic representation [Figure 8(c)].

Figure 8(d) shows the comparison of structures height at different separation distances. The height is uniform while the separation distance between structures is higher than 170 μm, demonstrating that trapezoidal shape is not a limitation for PDMS device fabrication. Recently, Kang et al.[38] reported SU-8 structures with this shape for the fabrication of a microfluidic neuron culture device.

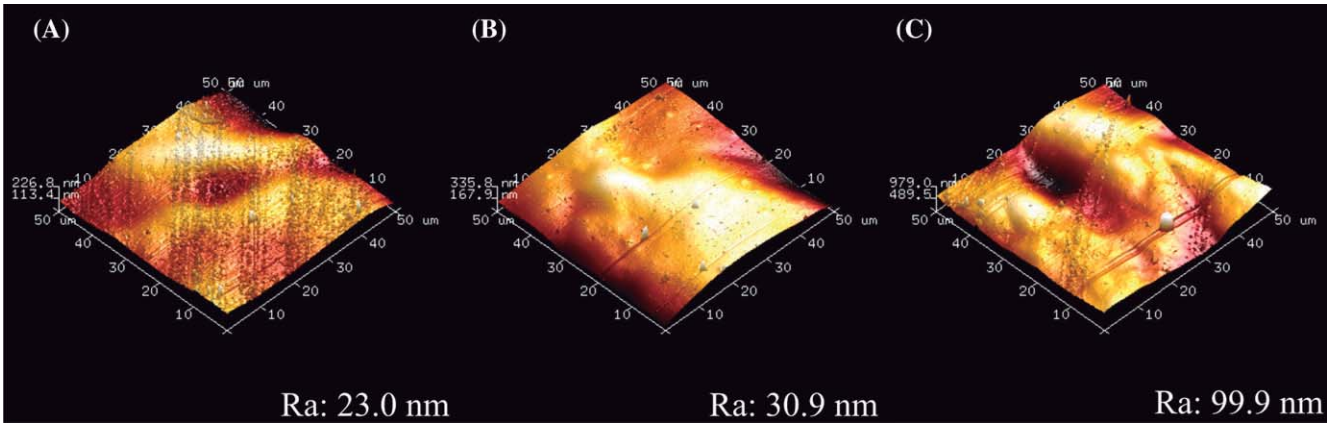

FIGURE 4 AFM images of molds surface. Ra represents the average roughness value. UVA exposure time on reverse side: A: 35 s, B: 40 s, and C: 48 s. [Color figure can be viewed at wieyonlinelibrary.com]

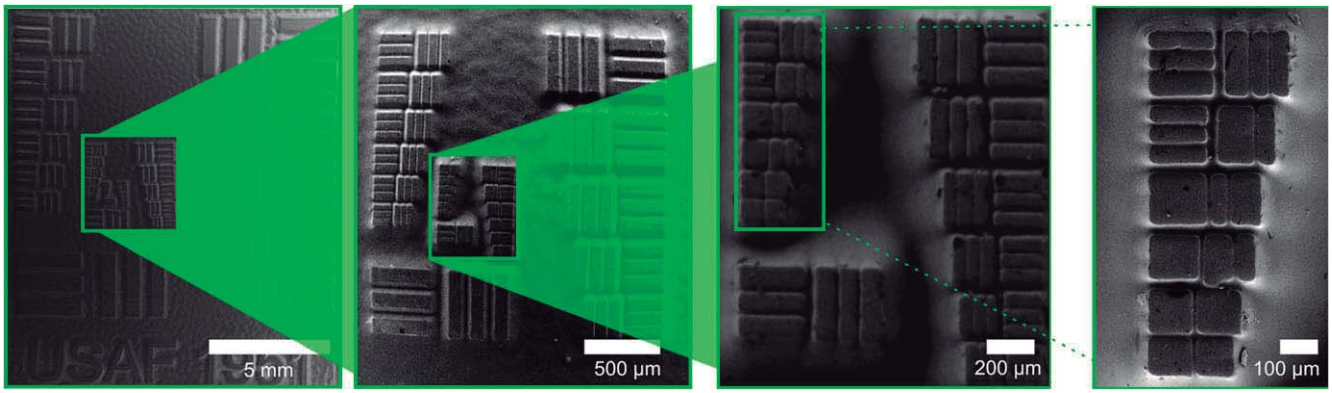

FIGURE 6 SEM images of structures embossed from Fmold. Fabrication conditions: first step—UVA exposure time on reverse side = 54 s, UVA front side exposure = 360 s. [Color figure can be viewed at wieyonlinelibrary.com]

In summary, the results demonstrate that with the proposed technology it is possible to obtain Fmolds with different channel dimensions (length, width, and height). Structures with a minimum width of 25 µm and heights up to 1500 µm[23,39] could be made, achieving an aspect ratio of 60. Regarding the length, it is possible to make multiple molds with a wide variety of dimensions. In addition, it is important to highlight that they can be manufactured up to a total size of 1270 × 2062 mm^2 (graphical abstract image).[40] Fmolds characterization with height structures in the millimeter scale will be the aim of future work.

PDMS Microdevices Fabrication

The Fmold fresh template and Fmold treated with SiO_2 (Fmold-T) were evaluated to optimize PDMS microdevice fabrication. The Fmold was fabricated using a design that contains homogeneous squares with dimensions of 1000 µm and separation between structures of 400 µm. Several replicates can be obtained using the same Fmold; however, PDMS residues are adhered to the mold as a result of the affinity between the Flexcel polymer and PDMS [Figure 9(a)]. To solve this problem, an SiO_2 coating was performed. Consequently, using Fmold-T, an adequate demolding was obtained and no residues of adhered PDMS were observed [Figure 9(b)]. This is because the SiO_2 thin film deposited on the Fmold-T avoids undesirable stickiness between the PDMS and the mold. As alternative to the PDMS microdevices fabrication process using Fmold-T technique, epoxy resin replicas from the Fmold were tested (Figures S2 and S3).

It is known that silanization treatment with trichloro (1H,1H,2H,2H-perfluorooctyl)silane on a silicon surface is a common method to facilitate the demolding process of the PDMS microdevices as well as to protect the integrity of the master mold. The coupling of perfluorinated organosilane molecules to the silicon surface decreases its surface energy and promotes the release from the PDMS.[41,42] Therefore, a silanization treatment of the Fmold-T was performed. Two treatments of silanization-exposure times under vacuum were tested, at 1 and 3 h. Because no differences were found with both treatments, the Fmold-T was silanized using the shortest time.

To demonstrate the replication fidelity of our method, 50 PDMS replicas were fabricated using the same Fmold-T. Figure 10 (a) shows the binocular magnifier images of Fmold at the 1st, 4th, 8th, and 50th PDMS replicas. For the replicas, it was used a design with heterogeneous squares. Figure 10(b) shows the height measurements recorded by profilometry from the Fmold-T and PDMS replicas. The comparison between the structure dimensions of the Fmold-T and the PDMS replicas indicates that the height and depth vary less than 10%, which demonstrates

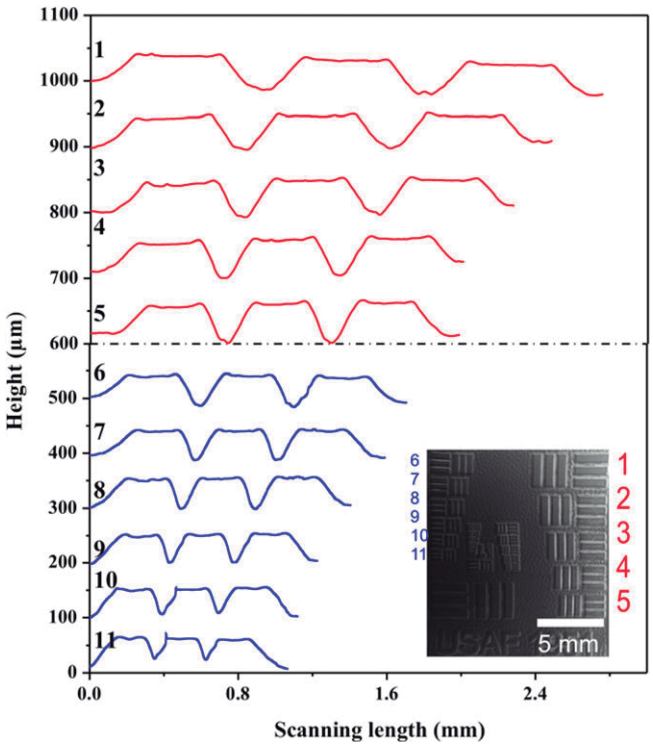

FIGURE 7 Height measurements of Fmold recorded by profilometry. SEM image appears on the right side. Fabrication conditions: first step—UVA exposure time on reverse side = 54 s, UVA front-side exposure = 360 s. Height measurements were determined by profilometry technique (n = 3). [Color figure can be viewed at wieyonlinelibrary.com]

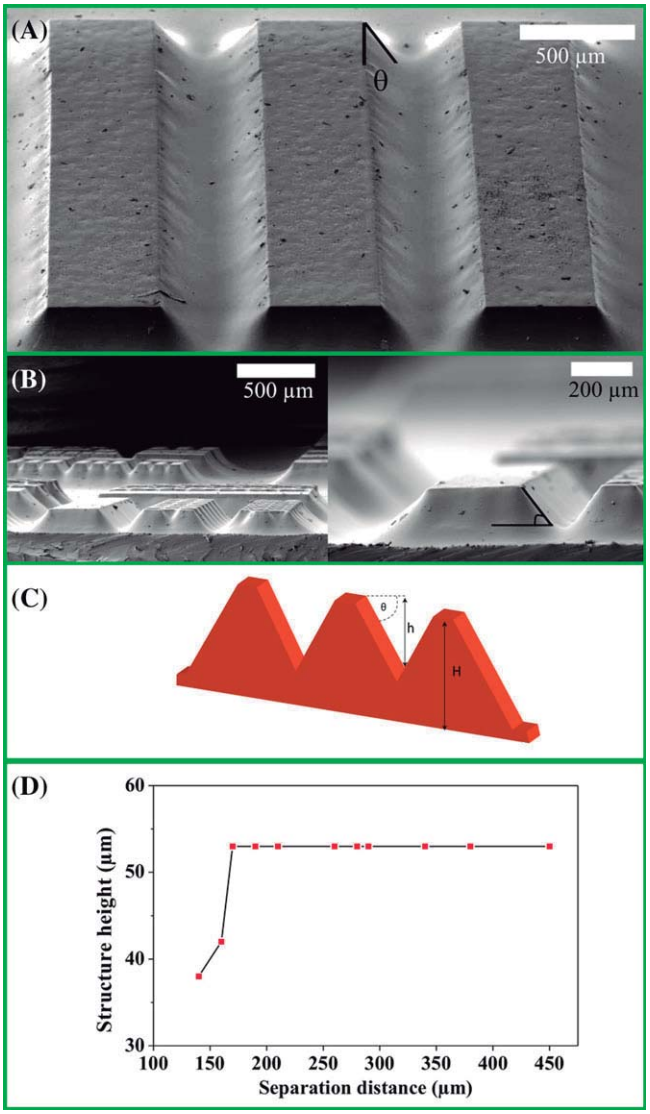

FIGURE 8 (A, B) SEM images of the cross section of Fmold, (C) schematic representation of the resulting structures height from overlapping, and (D) structures height at different separation distance. [Color figure can be viewed at wieyonlinelibrary.com]

that PDMS can be replicated with high fidelity, being these values comparable to typical in-plane photolithographic tolerances of approximately 10%.[4] High fidelity of replication was also observed in the analysis of Fmold-T and PDMS replica of a standard test target USAF 1951 by SEM and profilometry. Comparison of width, height, and depth of channels shows a low variation (<10%) on the entire range of the channels (Figure S4 and Table S1). Furthermore, the reusability and durability of the Fmold-T was the Fmold-T can be used many times to get PDMS replicas without apparent degradation in featured mold dimensions, and therefore decreasing the manufacturing costs.

It is well known that molds made in silicon wafers with photoresin have a limited lifetime[3] because structures created with this material are prone to be released from the wafer. In the case of the Fmold-T, the mold with the structures of interest forms a single element, thus, there is no possibility of detachment of the structures. Furthermore, the inclination of the sidewalls can reduce postdetachment contact and frictional resistance between the replicated structure (PDMS) and Fmold-T, allowing a better demolding.[43] This fact is an advantage especially when the structures formed in the mold have a high aspect ratio. In the case of SU-8 resin, mold angles are smaller than 90° and present difficulties in the demolding process. This is why the SU-8 resin tends to be delaminated from the support (generally silicon wafers), especially when the structures have a high aspect ratio.[44]

Devices fabrication through printing plate photopolymers have been described previously.[16,45,46] However, to the best of our knowledge, the methodology developed in this work shows for the first time the fabrication of photopolymer master molds reaching sizes up to 1270 × 2062 mm^2, at low cost and commercially available worldwide.

PDMS Device Applied to Fluid Injection and EOR Analysis

Several studies of microfluidic systems for EOR have been developed up to date. The assays have been performed with different chemical compounds such as surfactant/water floods,[47] polymer floods such as HPAM,[48] foam floods,[49] nanofloods with nanoparticles,[50] or micromodels to simulate the processes of microbial EOR.[51] In this paper, the functionality of the EOR microdevice was evaluated injecting, oil, water, and a commercial polyacrylamide polymer.

The microdevice was fully injected with crude oil at a flow rate of 1.0 mL h^{-1} until it was successfully trapped in the pore

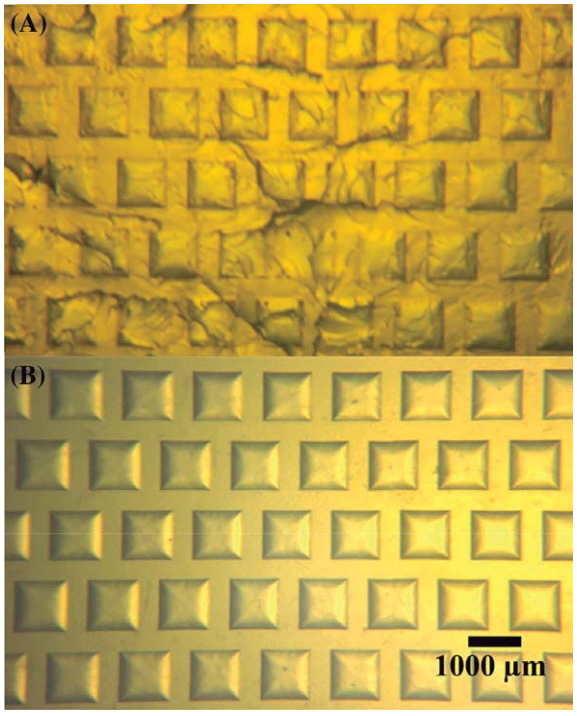

FIGURE 9 Images of Fmold obtained after PDMS replica manufacturing. (a) Fmold (fresh template) and (b) F-mold-T coated with SiO_2. [Color figure can be viewed at wieyonlinelibrary.com]

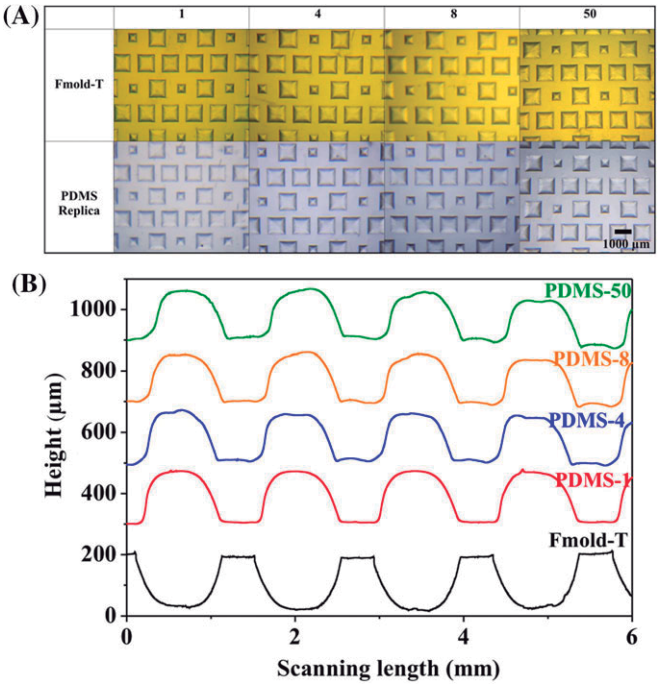

FIGURE 10 PDMS replication using Fmold-T master mold. (a) Binocular magnifier images and (b) Height measurements recorded by profilometry of Fmold-T at the 1st, 4th, 8th, and 50th PDMS replicas. Fabrication conditions: first step—UVA exposure time on reverse side = 42 s. (Scale bar: 1000 μm.) Height measurements were determined by profilometry technique ($n = 3$). [Color figure can be viewed at wieyonlinelibrary.com]

space; the next step was the injection of water at a flow rate of 0.5 and 2.0 mL h^{-1} to reach residual oil saturation. Then, polyacrylamide polymer solution (1000 ppm) was injected at 0.5 and 1.0 mL h^{-1}. Standard image analysis using Image J was used to determine the percentage of oil recovered. The difference between the initial state of the black pixels and the final state was interpreted as oil recovery.

Figure 11 displays the oil recovery in relation with PV and the images obtained in each stage, which shows water and polymer flowing into the pore space and displacing crude oil. It is obvious that water injection at a flow rate of 0.5 mL h^{-1} displaces the crude oil from the channels, giving an oil recovery of 37% (1.25 PV), when the flow rate increases at 2.0 mL h^{-1}, the oil recovery raises to 46% (4 PV). Moreover, polymer flooding recovery was 5% (6.1 PV) at a flow rate of 0.5 mL h^{-1} and 21% (8 PV) at a flow rate of 1.0 mL h^{-1}, giving a total 21% of oil recovery. The total oil recovery achieved was 67%. The liquids flooding in the microfluidic device has been included in supporting information (Video S1).

Comparison of Availability, Costs, and Resolution of Different Mold Manufacturing Technologies

It is well known that developed countries have a higher index of laboratories and publications in almost all areas of science than developing countries. In case of microfluidics, this effect is particularly marked, because the fabrication of devices of quality and good resolution, it is necessary to have an expensive equipment to manufacture the photomasks and molds. While the SU-8 mold cost is relatively low for research groups with manufacturing facilities (without considering cleanroom maintenance expenses and equipment amortization), the cost of acquiring SU-8 molds is very high for research groups with no manufacturing equipment.

Due to their high cost, these facilities are practically nonexistent throughout the southern hemisphere. For example, in the country where this article is generated, there are only three cleanrooms, which are not always available for research groups outside the institution. One option to carry out the assays would be to hire the service of chips manufacturing outside the country, but there are few companies or universities in the whole planet offering this service. The price of a SU-8 mold charged by these companies is between £375 and £525, depending on the required resolution (Quote by FlowJEM). These prices are too high for research laboratories in developing countries, where grants awarded on average do not exceed £3000 per year.[52]

As a result of the previously mentioned, throughout the southern hemisphere, there are only 8 of a total of 344 reported research groups investigating microfluidics.[53] Something similar happens with microfluidics companies, finding only one in the whole southern hemisphere.[54]

The method proposed in this work will provide great advances in the field of microfluidics because it will allow to all laboratories the ability to work in the area of microfluidics (including those in developing countries) without the needs of micromanufacturing facilities or equipment to create a master mold. The Flexcel technology can be commercially obtained at much lower cost than SU-8 molds, it is commonly used in the graphics industry and it can be acquired worldwide (including no developing countries). Regarding the availability, in contrast to the only 20 companies or universities offering photolithography services, there are now more than 400 companies distributed in 60 countries offering Fmold manufacturing services.[55] Regarding the costs, a FMold of 220 × 350 mm^2, costs

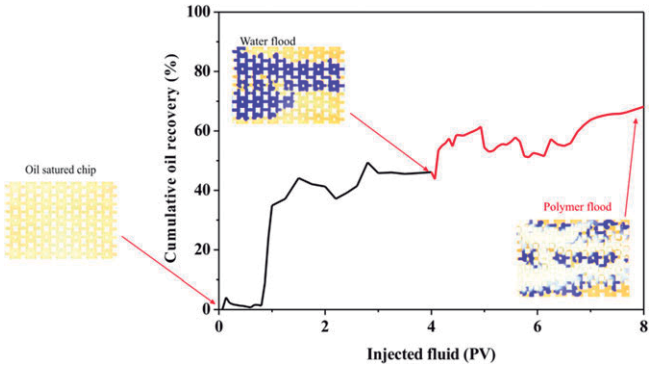

FIGURE 11 Oil recovery analysis. Cumulative oil recovery as a function of PV and images of oil saturated, dyed water flood, and polymer flood. [Color figure can be viewed at wieyonlinelibrary.com]

£28 in Argentina[56] and £40 in Spain.[57] These prices are at least 10 times less expensive than SU-8 commercial molds, and more accessible to developing laboratories.[58]

At present, there are other alternative methodologies to SU-8 molds, some of which are shown in Table 1. Nevertheless, most of these techniques do not achieve the resolution of the photoresin or the processes are expensive and inaccessible, therewith the traditional technique of photoresin molds is still the most used in microfluidics.

Table 1 shows a comparison of the minimum channel width achieved by Fmold and other nontraditional methods of microfluidic molds fabrication. These values range between 21 and 200 μm, and therefore the minimum channel width obtained in this work is well suited for microfluidic devices manufacturing.

3D printing is one of the best-known alternative techniques; however, until now, its applicability is limited in part by the technical inability to print reliable microfluidic channels with dimensions less than several hundreds of microns in a reasonable sized device[34,61] at a reasonable price. Among the main disadvantages of 3D printing can be mentioned the difficulties on the removal of the support material from small fluidic features, a relatively wasteful print process and channels with rough surfaces.[34]

There is a great number of 3D printing equipment that allows molds or chips previously reported in the literature. However, when the cost of equipment falls, the channel resolution obtained falls as well. For example, the cost of PDMS-chip produced by 3D printing was reported as £1.50 but with a minimal cross-sectional area of 200 μm.[62]

High resolution channels obtained by 3D printing have been reported in some research works, but the cost of the equipment is very high (EnvisionTEC, £74.900, resolution: 16 μm),[63] or the equipment is homemade manufactured.[64] In both cases, the molds produced are not commercially available at global level, as in the case of FMold.

TABLE 1 Minimum Channel Widths of Nontraditional Methods of Microfluidic Molds Manufacture

Mold technique	Channel width (μm)	Reference
Stainless steel stamp	21	14
Fmold	25	This work
Toner	26.6	6
Liquid molding	40	10
3D printing	45	59
Liquid molding	60	9
Building blocks	100	5
Laser ablation	120	11
Semi-contact writing	140	13
Laser swelling	190	12
3D printing	200	34,60
WAX mold	200	8

It is also possible to achieve structures reaching widths on the nanometric scale using conventional photoresins, under a high resolution exposure with quartz or glass masks, and under electron beam lithography or focus ion beam.[65] Several studies combining the Flexcel polymer with these techniques in order to reach the minimum width will be the subject of future work. In this work, a minimum width of 25 μm was achieved, which allows Flexcel technology to be promising to manufacture conventional microfluidic devices at low cost, which normally have channels with width greater than 100 μm. Therefore, it is thought that the proposed innovative methodology could give a breakthrough to the development of microfluidics and lab-to-chip technologies.

CONCLUSIONS

The Fmold provides a good alternative to conventional microfluidic manufacture methods of photoresin over silicon wafers. The fidelity of replication, stability, and durability of the Fmold were proved. It can be used multiple times with the acquisition of reliable replicas, without delamination, since the mold and the structures designed compose a unique piece. This method allows the manufacture of microfluidic molds achieving very large dimensions (1270 × 2062 mm^2), reaching a minimum structure size of 25 μm and structures height ranging from 53 to 1500 μm. To the best of our knowledge, no material or technology with these characteristics has been reported yet for the use as a mold for the manufacture of microfluidic devices, which allows the integration of multiple laboratory functions and detection systems in a single layer. Another advantage of this technology is that the Fmolds can be commercially obtained at much lower cost than SU-8 molds. In addition, since Flexcel technology is commonly used in the graphics industry, Fmolds can be acquired worldwide.

It is possible to infer that the new methodology of microfluidic chips fabrication shown in this article will help a positive evolution in the microfluidic field, serving as support for many laboratories lacking of micromanufacturing facilities, such as those related to biology and chemistry fields, especially in microfluidic laboratories from developing countries.

ACKNOWLEDGMENTS

The authors would like to thank the financial support from CONICET (PIP2015), ANPCyT (PICT-STARTUP 3772) and Florencio Fiorini grant. We would like to thank Andrea Vaca (ESPE), Alexis Debut (ESPE), Claudio Ferrari (CNEA), Cintia Notcovich (CNEA), Jorge. L. Fernandez, Pamela Schreiber, Claudio Acosta (Kodak Argentina S.A.I.C.), Ezequiel Rodriguez (E-magen SA), and Francisco Villalba (E-magen SA) for general support and discussion.

REFERENCES

1 A. Bubendorfer, X. Liu, A. V. Ellis, *Smart Mat. Struct.* **2007**, *16*, 367.

2 D. C. Duffy, J. C. McDonald, O. J. A. Schueller, G. M. Whitesides, *Anal. Chem.* **1998**, *70*, 4974.

3 B. H. Jo, L. M. Van Lerberghe, K. M. Motsegood, D. J. Beebe, *J. Microelectromech. Syst.* **2000**, *9*, 76.

4 S. P. Desai, D. M. Freeman, J. Voldman, *Lab Chip* **2009**, *9*, 1631.

5 M. A. Stoller, A. Konda, M. A. Kottwitz, S. A. Morin, *RSC Adv.* **2015**, *5*, 97934.

6 C. J. Easley, R. K. P. Benninger, J. H. Shaver, W. Steven Head, D. W. Piston, *Lab Chip* **2009**, *9*, 1119.

7 C. Chung, Y.-J. Chen, P.-C. Chen, C.-Y. Chen, *Int. J. Precis. Eng. Manuf.* **2015**, *16*, 2033.

8 Z. Li, L. Hou, W. Zhang, L. Zhu, *Anal. Methods* **2014**, *6*, 4716.

9 X. Liu, Q. Wang, J. Qin, B. Lin, *Lab Chip* **2009**, *9*, 1200.

10 L. Yang, L. Zhu, Z. Li, B. Lu, *Multimed. Tools Appl.* **2018**, *77*, 3761.

11 Z. Isiksacan, M. T. Guler, B. Aydogdu, I. Bilican, C. Elbuken, *J. Micromech. Microeng.* **2016**, *26*, 35008.

12 E. Joanni, J. Peressinotto, P. S. Domingues, G. de Oliveira Setti, D. P. de Jesus, *RSC Adv.* **2015**, *5*, 25089.

13 L. Gutzweiler, F. Stumpf, L. Tanguy, G. Roth, P. Koltay, R. Zengerle, L. Riegger, *J. Micromech. Microeng.* **2016**, *26*, 45018.

14 J. Kotowski, D. Šnita, *Microelectron. Eng.* **2014**, *125*, 83.

15 M. De Volder, S. H. Tawfick, S. J. Park, D. Copic, Z. Zhao, W. Lu, A. J. Hart, *Adv. Mater.* **2010**, *22*, 4384.

16 A. W. Browne, M. J. Rust, W. Jung, S. H. Lee, C. H. Ahn, *Lab Chip* **2009**, *9*, 2941.

17 A. Carlson, A. M. Bowen, Y. Huang, R. G. Nuzzo, J. A. Rogers, *Adv. Mater.* **2012**, *24*, 5284.

18 C. A. Conn, K. Ma, G. J. Hirasaki, S. L. Biswal, *Lab Chip* **2014**, *14*, 3968.

19 M. Schneider, Wettability Patterning in Microfluidic Systems and Applications in the Petroleum Industry. Ph.D. Thesis, University Pierre & Marie Curie, Paris, February 2011.

20 N. K. Karadimitriou, S. M. Hassanizadeh, *Vadose Zo. J.* **2012**, *11*, 128.

21 V. A. Lifton, *Lab Chip* **2016**, *16*, 1777.

22 D. Novaković, S. Dedijer, S. Mahović Polja, *Tech. Gaz.* **2010**, *17*, 403.

23 Kodak, Flexcel SRH Flexographic Plates, http://www.ratcliffe-sa.com.ar/documentos/Kodak_Flexcel_SRH.pdf (accessed Feb 1, 2018).

24 T. Tomašegović, S. M. Poljaček, M. Leskovac, *J. Appl. Polym. Sci.* **2016**, *133*, 43526.

25 R. Knoll, U.S. Patent US 2002/0001775 A1 photopolymerizable Flexographic Printing Elements Comprising SIS/SBS Mixtures as Binder for the Productionof Flexographic Printing Plates, **2002**, *January 3*, 2002

26 KLayout - High Performance Layout Viewer and Editor, http://www.klayout.de/index.php (accessed Feb 1, 2018).

27 C. Lasorsa, P. J. Morando, A. Rodrigo, *Surf. Coat. Technol.* **2005**, *194*, 42.

28 A. Peñaherrera, C. Payés, M. Sierra-Rodero, M. Vega, G. Rosero, B. Lerner, G. Helguera, M. S. Pérez, *Microelectron. Eng.* **2016**, *158*, 126.

29 J. Schindelin, I. Arganda-Carreras, E. Frise, V. Kaynig, M. Longair, T. Pietzsch, S. Preibisch, C. Rueden, S. Saalfeld, B. Schmid, J. Y. Tinevez, D. J. White, V. Hartenstein, K. Eliceiri, P. Tomancak, A. Cardona, *Nat. Methods* **2012**, *9*, 676.

30 H. Zeng, *Polymer Adhesion, Friction, and Lubrication*, John Wiley & Sons, New Jersey, **2013**.

31 R. A. Wolf, *Plastic Surface Modification*, Carl Hanser Verlag, Munich, **2010**.

32 F. Walther, T. Drobek, A. M. Gigler, M. Hennemeyer, M. Kaiser, H. Herberg, T. Shimitsu, G. E. Morfill, R. W. Stark, *Surf. Interface Anal.* **2010**, *42*, 1735.

33 G. D. Hoople, D. A. Rolfe, K. C. McKinstry, J. R. Noble, D. A. Dornfeld, A. P. Pisano, *J. Micro. Nano-Manuf.* **2014**, *2*, 34502.

34 S. Waheed, J.-M. Cabot Canyelles, N. Macdonald, R. M. Guijt, T. Lewis, B. Paull, M. C. Breadmore, *Lab Chip* **2016**, *16*, 1993.

35 M. I. Mohammed, M. N. H. Zainal Alam, A. Kouzani, I. Gibson, *J. Micromech. Microeng.* **2017**, *27*, 15021.

36 E. F. GLYN, USAF 1951 and Microcopy Resolution Test Charts. efg's, Tech. http://www.efg2.com/Lab/ImageProcessing/TestTargets (accessed Feb 1, 2018).

37 X. Liu, J. T. Guthrie, C. Bryant, *Surf. Coat. Int.: B Coat. Trans.* **2002**, *85*, 313.

38 M. Kang, J. H. Byun, S. Na, N. L. Jeon, *RSC Adv.* **2017**, *7*, 13353.

39 Kodak, Flexcel NX. https://www.kodak.com/uploadedFiles/Flexcel NXC Plates brochure.pdf, 2017 (accessed Feb 1, 2018).

40 Kodak, DITR film. https://www.kodak.com/PK/en/print/Products/Flexographic/KODAK_DITR_Film/default.htm (accessed Feb 1, 2018).

41 B. Bhushan, D. Hansford, K. K. Lee, *J. Vac. Sci. Technol. A* **2006**, *24*, 1197.

42 S. Guilles, *Chemical Modification of Silicon Surfaces for the Application in Soft Lithography*, Zentralbibliothek Jülich, Jülich, **2007**.

43 J. Zhang, M. B. Chan-Park, S. R. Conner, *Lab Chip* **2004**, *4*, 646.

44 S.-J. Kim, H. Yang, K. Kim, Y. T. Lim, H.-B. Pyo, *Electrophoresis* **2006**, *27*, 3284.

45 J. Olkkonen, K. Lehtinen, T. Erho, *Anal. Chem.* **2010**, *82*, 10246.

46 S. Kim, H. Sojoudi, H. Zhao, D. Mariappan, G. H. McKinley, K. K. Gleason, A. J. Hart, *Sci. Adv.* **2016**, *2*, 1.

47 K. He, L. Xu, Y. Gao, K. B. Neeves, X. Yin, B. Bai, Y. Ma, J. Smith, SPE Improved Oil Recovery Symposium, Society of Petroleum Engineers, Tulsa, Oklahoma, USA. 12-16 April, **2014**.

48 A. M. Howe, A. Clarke, D. Giernalczyk, *Soft Matter* **2015**, *11*, 6419.

49 L. Hendraningrat, S. Li, O. Torsater, *OnePetro* **2013**, *3*, 2229.

50 H. ShamsiJazeyi, C. A. Miller, M. S. Wong, J. M. Tour, R. Verduzco, *J. Appl. Polym. Sci.* **2014**, *131*, 40576.

51 H. Khajepour, M. Mahmoodi, D. Biria, S. Ayatollahi, *J. Petrol. Sci. Eng.* **2014**, *120*, 10.

52 CONICET, convocatorias.conicet, http://convocatorias.conicet.gov.ar/investigacion-y-desarrollo/ (accessed Feb 1, 2018).

53 O. International, Microfluidics research groups, http://research.omicsgroup.org/index.php/List_of_microfluidics_research_groups (accessed Feb 1, 2018).

54 Fluidicmems, List of microfluidics lab on a chip and biomems companies, http://fluidicmems.com/list-of-microfluidics -lab-on-a-chip-and-biomems-companies (accessed Feb 1, 2018).

55 L. Graafine, Changed the capabilities of flexo printing, http://www.lahdengraafinen.fi/File/NX_Overview.pdf?427393 (accessed Feb 1, 2018).

56 Flexoemagen, Digital photopolymers, http://www.flexoemagen.com.ar/ (accessed Feb 1, 2018).

57 Troflex, Digital photopoymers, http://www.troflex.com/ (accessed Feb, 2018).

58 Flowjem, Polymer microfluidic tehnology, http://www.flowjem.com/ (accessed Feb, 2018)

59 K.-I. Kamei, Y. Mashimo, Y. Koyama, C. Fockenberg, M. Nakashima, M. Nakajima, J. Li, Y. Chen, *Biomed. Microdevices* **2015**, *17*, 36.

60 N. Bhattacharjee, A. Urrios, S. Kang, A. Folch, *Lab Chip* **2016**, *16*, 1720.

61 Y. Hwang, O. H. Paydar, R. N. Candler, *Sens. Actuat. A-Phys.* **2015**, *234*, 65.

62 S. Mohammadi, M. Masihi, M. H. Ghazanfari, *Transp. Porous Media* **2012**, *91*, 973.

63 P. F. O'Neill, A. Ben Azouz, M. Vázquez, J. Liu, S. Marczak, Z. Slouka, H. C. Chang, D. Diamond, D. Brabazon, *Biomicrofluidics.* **2014**, *8*, 52112.

64 W. Lee, V. Lee, S. Polio, P. Keegan, J. H. Lee, K. Fischer, J. K. Park, S. S. Yoo, *Biotechnol. Bioeng.* **2010**, *105*, 1178.

65 C. Duan, W. Wang, Q. Xie, *Biomicrofluidics* **2013**, *7*, 26501.